Doppler Global Velocimetry
A New Way to Look at Velocity

James F. Meyers
NASA - Langley Research Center
Hampton, Virginia 23665

and

Hiroshi Komine
Northrop Corporation
Research and Technology Center
Palos Verdes Peninsula, California 90274

ASME Fourth International Conference on
Laser Anemometry
August 3-9, 1991
Cleveland, Ohio

Doppler Global Velocimetry
A New Way to Look at Velocity

James F. Meyers
NASA - Langley Research Center
Hampton, Virginia 23665

and

Hiroshi Komine
Northrop Corporation
Research and Technology Center
Palos Verdes Peninsula, California 90274

Abstract

A new laser velocimetry technique, Doppler global velocimetry, is described. This technique is capable of simultaneously measuring in real time the three components of velocity of an entire particle field illuminated by a laser light sheet. A prototype one-component velocimeter is described along with the signal processing electronics. The system was tested by measuring the velocity field from a rotating wheel and a small subsonic jet flow in the laboratory. The first wind tunnel test measured the vortical velocity field above a delta wing. The results are presented and compared with fringe-type laser velocimeter and five-hole probe data.

Introduction

The development of measurement technology, like many other technologies, is driven by the needs of potential users. Airplane designs were first studied by trial and error flight testing, but being too expensive and dangerous, wind tunnels were developed to investigate the performance of proposed airplane designs. Since a pilot could not fly the wind tunnel model and get a *feel* of the aircraft performance, instrumentation was developed to obtain the data needed to assess the performance of the proposed design. Instruments such as Pitot probes and hot wires were developed to measure the flow velocity. These techniques worked well and were used to support the design of many an airplane, however the disturbance of the flow created by the physical presence of the instrument led to concern over the measurement accuracy. Nonintrusive techniques such as shadowgraphy and Schlieren provided views of the air flow especially shock waves, but

yielded little quantitative data. The advent of the laser allowed the development of laser velocimetry, a technique which measures the velocity at a point within the flow to a high accuracy without disturbing it. Shortly after this development, computational fluid dynamics research upped the ante by requiring velocity measurements throughout the flow, preferably simultaneously. Laser velocimetry measurements over a detailed grid required hours of wind tunnel time which place a strain on the assumption of flow stationarity. In response to these issues, particle image velocimetry was developed. This technique uses a photographic camera to obtain a double exposure of the particle field within the flow using a double pulsed laser light sheet. While this technique obtains the simultaneous measurement of velocities over the viewing area, it has four drawbacks: limited viewing area (typically 4 x 5-inches), limited to two velocity component measurements, directional ambiguity, and long data processing times. Although these drawbacks may be reduced, or in some cases even eliminated with further research, a new technique—Doppler Global Velocimetry—is proposed which has the advantage of particle image velocimetry without its drawbacks.

The Basic Principle

In the manner of particle image velocimetry, PIV, the Doppler global velocimeter, DGV, uses a laser light sheet to illuminate a particle field within the flow to simultaneously make multiple velocity measurements. Instead of measuring the time-of-flight between multiple exposures of the particle field, the DGV measures the Doppler shift of light scattered from the illuminated particles. This approach improves on PIV by providing the capability to measure the full three-component velocity field without directional ambiguity.

The velocity component measured is determined by the placement of the laser light sheet and the receiving optical system. If the propagation direction of the laser light sheet is represented by the unit vector $\hat{\imath}$, and the propagation direction of the collected scattered light represented by the unit vector $\hat{o}$, the velocity component measured is parallel to the difference between these two unit vectors, $\hat{o} - \hat{\imath}$. As shown in figure 1, the measured velocity vector, $\hat{o} - \hat{\imath}$, is the vector perpendicular to the bisector of vectors $\hat{o}$ and $\hat{\imath}$ lying within the plane defined by the vectors $\hat{o}$ and $\hat{\imath}$. Thus for a general flow velocity vector $\mathbf{V}$, the shift in frequency, $\Delta\nu$, of the collected scattered laser light is dependent on the vectorial dot product between the velocity vector $\mathbf{V}$ and the measurement vector $\hat{o} - \hat{\imath}$ as shown in equation 1:

$$\Delta\nu = \frac{\nu_o\,(\hat{o}-\hat{i})\bullet V}{c} \qquad (1)$$

where ν_o is the optical frequency of the laser light sheet and c is the speed of light. Obviously, in a global measurement the exact measurement vector is dependent on the specific pixel in the CCD camera and the propagation vector of the laser light viewed by that pixel. Therefore, the transfer function described by equation 1 must be evaluated for each pixel within the viewing camera. Three-component measurements are possible by selecting three observation directions, $\hat{o}_1$, $\hat{o}_2$, and $\hat{o}_3$, or selecting three propagation directions of the laser light sheet, $\hat{i}_1$, $\hat{i}_2$, and $\hat{i}_3$.

Classic approaches to measure the Doppler frequency shift of scattered light in laser Doppler velocimetry include heterodyne detection (Yeh and Cummins, 1964) to mix shifted scattered light with unshifted reference light to obtain the difference (Doppler) frequency, and Fabry-Perot interferometry (Self, 1974) to measure the shift in scattered light frequency directly. These techniques are not applicable to global measurements since their allowable acceptance angle (Huffaker, et al, 1969) is too limited. The use of a Michelson interferometer can increase the allowable acceptance angle and has been used for global applications (Seiler and Srulijes, 1986). This technique provides fringe maps of constant phase shift between direct and time delayed collected scattered light. These fringes indicate locations where the Doppler shifts in the scattered light are multiples of the time delay in the interferometer. The difficulty in maintaining alignment of the interferometer and the still relatively narrow acceptance angle limit the application of this technique. Further, the required optical precision within the interferometer make subsonic measurements very difficult because of the small phase shifts obtained from low velocities.

Doppler global velocimetry uses the edge of an absorption line in molecular Iodine to serve as a frequency discriminator to directly measure the Doppler shift of the collected scattered light (Komine, et al, 1991). An Argon ion laser operating in single-line mode at 514.5 nm is tuned by tilting the intercavity etalon to an optical frequency corresponding to a point midway along the edge of an absorption line of an Iodine absorption line filter (ALF), figure 2. Collected scattered light from a stationary object or cloud of particles will be attenuated by 50 percent as it passes through the ALF. If the object or particle cloud is moving, the attenuation through the ALF will increase (or decrease, depending on the direction of movement) by an amount proportional to the Doppler shift. By using the ALF as a filter for a CCD camera, an entire laser light sheet can be viewed and the velocity field determined.

In practice, particle size distribution and number density, and the laser light sheet intensity profile are other factors influencing the amount of collected scattered light reaching the viewing camera. These influences can be minimized by viewing the same scene with a second camera without an ALF, figure 3, to provide a reference signal used to normalize the viewing camera output. The two cameras must be aligned with corresponding pixels in each camera viewing the same portions of the light sheet. Other influences from nonuniform optical elements and variations in pixel sensitivities in the CCD cameras are removed using pixel-by-pixel ratio calibrations.

Signal Processing

The signal processing electronics must perform three tasks: synchronize the cameras, normalize the signal camera output, and apply pixel sensitivity corrections. The camera synchronization circuit forces the signal camera and reference camera to simultaneously output signals from corresponding pixels. Two normalization circuits have been constructed—a low quality, real time analog circuit and a prototype high quality, but slow digital circuit. The pixel sensitivity corrections are applied following data transfer to the computer.

The effects of particle size distribution and number density and variations in the input laser power distribution can be minimized only if corresponding pixels in the two cameras collect light originating from the same volume within the light sheet during the same period of time. Precise optical alignment including identical magnification by each camera lens is required to insure viewing of identical measurement volumes by each pixel pair. Normally, two cameras are synchronized by using the internal pixel clock from the master camera to drive the slave camera. However, the time delay in driving the second camera is too long to obtain the necessary precise pixel synchronization. Therefore the internal pixel clocks were disabled and an external clock synchronization circuit used to simultaneously drive both cameras. This results in simultaneous interrogation of corresponding pixels in each camera to obtain identical views in time of the scattered light.

Normally, the video output from a camera is transferred to a computer by using a digital frame grabber. The image can then be processed further within the frame grabber and the results stored on disk. Up to 16 frames can be obtained in real time before acquisition must be suspended for processing and storage. However, the use of two cameras adds greater complexity. Not only are two frame grabbers required, but they must be synchronized to align corresponding pixels. The data from each frame grabber must then be transferred to the computer for the

required image normalization. Therefore it is not possible to obtain real time operation using this method.

An alternate approach is to construct a specialized dual frame grabber designed specifically to acquire synchronized images from two cameras and to perform the normalization operation. A prototype dual frame grabber has been constructed based on the block diagram shown in figure 4. The synchronized image from each camera is digitized by an 8–bit analog-to-digital converter, ADC. The two synchronized ADC's are operated at 10 MHz to obtain 512 x 480 pixel mappings of the images. Since the ADCs are 8-bit, there are 256 possible values and 256^2 or 65,536 possible results from a normalization operation. Therefore, the most time efficient method of dividing the signal image by the reference image is to use a lookup table containing all possible quotients. The signal ADC provides the row address and the reference ADC provides the column address to select the appropriate cell within the lookup table. Maximum accuracy is obtained from the 8-bit lookup table by assuming that the signal output will always be less than the reference output. This assumption allows the quotient values from 0 to 1.0 to be mapped to integer values of 0 to 255.

The prototype dual frame grabber transfers the output from the lookup table to the controlling computer via an IEEE-488 interface for further processing. The acquisition and processing of an image requires 30 seconds and is thus unacceptable for real time operation. The next phase is to include a high-speed multiplier synchronized to a pixel mapping lookup table to correct the output ratios for pixel sensitivity variations. The corrected ratios are then transferred to the controlling computer via IEEE-488 in DMA mode for digital storage of selected images. Real time operation is obtained by converting the corrected digital ratios to false color images and then to analog RGB for display and video recording on high resolution video recorders.

To obtain real time operation during the digital prototype stage, an analog normalization circuit was constructed which operated as an input stage to a standard computer frame grabber. The block diagram of the analog circuit is shown in figure 5. The video retrace synchronization pulse is removed from each of the two camera signals to prepare them for input to an analog divider. A known voltage replaces the reference signal if the signal approaches zero to keep the divider output within range. The divider output is converted back to a standard video signal by returning the stripped retrace synchronization pulse. This normalized video signal is passed to the frame grabber for conversion to false color and output as an RGB signal for display and recording. The frame grabber can also capture and store the image in a similar manner as the digital system.

Laboratory Experimentation

The ability of Doppler global velocimetry to make global measurements was tested in the laboratory. The tests consisted of measuring the velocity field of a rotating wheel and of a subsonic jet. The wheel was spun at various speeds to determine the response of the DGV. The velocity of the jet was also varied to determine the response to seeded gas flows.

The spinning wheel consisted of a flat blackened, 5-1/4-inch floppy disk which could be spun up to 18,500 rpm. The laboratory setup is illustrated in figure 6. The Argon ion laser was tuned to 514.5 nm with the specific optical frequency tuned with the etalon to nominally the 50 percent transmission point along the slope of the Iodine absorption line. As shown in figure 6, the input laser beam was aligned to be normal to the wheel and expanded to illuminate the entire wheel. With the receiver optical system located 45 degrees from the input laser beam, the nominal velocity component measured is 22.5 degrees from the wheel normal in the horizontal plane. The wheel was spun and the data acquired by the prototype digital dual frame grabber. The resulting gray scale version of a false color velocity map of the wheel spinning at 18,500 rpm is shown in figure 7a. A plot of the signal and reference amplitudes and the normalized signal along the vertical diameter of the wheel is shown in figure 7b. The signal and reference amplitudes clearly show the Gaussian behavior of the input laser beam as expected. This change in amplitude is removed by the ratio technique indicating that effects from variations in scattered light other than attenuation through the ALF have been removed.

The next laboratory test was to determine if the DGV could measure the velocity field of a seeded subsonic jet. The nominally 100 m/sec jet was seeded using a standard theatrical fogger and illuminated by a laser light sheet orientated vertically approximately 20 degrees from the streamwise flow direction. The receiver optics were placed normal to the streamwise flow direction within the horizontal plane containing the streamwise vector and the laser propagation vector. Thus the measured velocity component is in the horizontal plane in a direction 55 degrees from the streamwise flow direction as shown in figure 8. The resulting velocity map along with the centered horizontal velocity scan is shown in figure 9. The high velocity gradient on the left of the image corresponds to the narrow entrained region near the jet exit and the slow velocity reduction on the right corresponds to the length of the expanding entrained region illuminated by the light sheet, figure 8.

Wind Tunnel Experiments

The proof-of-concept test of the DGV in a wind tunnel was conducted in the Basic Aerodynamic Research Tunnel, BART. The vortical velocity field above a 75-degree delta wing was chosen as the test flow field since five-hole probe and fringe-type laser velocimeter investigations had been previously conducted in the tunnel on this model (Sellers and Kjelgaard, 1988; Meyers and Hepner, 1988). These measurements will be used as the comparative standards to determine the capabilities of the DGV. The model was placed at an angle of attack of 20.5 degrees to obtain a stable vortical flow field. The DGV was placed in the wind tunnel with the illuminating light sheet oriented normal to the surface of the model passing through the side of the tunnel. The receiver was placed in forward scatter, rotated 53 degrees from the propagation direction of the laser beam in the horizontal plane as seen in figure 3. This provided a measurement velocity vector in the horizontal plane, 26.5 degrees from the streamwise direction. The flow was seeded using the propylene glycol vaporization/condensation generator normally used for light sheet flow visualization in BART. The data acquisition consisted of obtaining 10 images at each measurement station using the digital dual frame grabber and averaging the images pixel-by-pixel to obtain the mean velocity flow field. Five minutes of real time data were also acquired using the analog normalization circuit coupled with a standard frame grabber to apply pseudo colors and conversion to NTSC video for recording.

The velocity flow field obtained from three component velocity measurements using the 5-hole probe and laser velocimeter with the tunnel Q set to 8.4 was resolved along the measurement direction of the DGV. The resolved measurements within the plane at the 70-percent chord location for an angle of attack of 20.5 degrees are presented in figures 10 and 11, respectively. The asymmetry of the velocity contours is due to the inclusion of a portion of the vortical rotation, (sin 26.5°), within the measurement direction. A single frame image obtained by the DGV at this chord location is presented in figure 12. The image has not been spatially rotated to remove the perspective view of the light sheet shown in figure 13 nor has any attempt been made to smooth the noise or remove the reflection of the light sheet from the model. The vortices are clearly seen with the expected velocity patterns. The 5-hole probe and laser velocimeter data indicate that velocity at the top of the left vortex should match the bottom of the right with the flow next to the wing being slightly higher due to flow compression. The top of the right vortex should likewise match the bottom of the left. This pattern is clearly illustrated in the single frame DGV results, figure 12. The velocity characteristics of the vortex flow can be seen by viewing the normalized signal amplitude (inversely proportional to velocity) profile

through the center of the two vortices, figure 14. (Note: The normalized signal amplitude is programmed to yield a full scale result if the signal amplitude is below threshold or the scattered light saturates the reference camera.) The high frequency oscillations in the profile are due mainly to sensitivity variations in the CCD elements of the camera. Averaging 10 frames of data removes turbulent flow variations and random noise leaving the fixed sensitivity variations visualized in the profile through the center of the vortices in figure 15. If the profile is high pass filtered, the variation due to pixel sensitivities can be isolated and used to develop a calibration to remove the variations. The resulting calibration is applied to the single frame profile shown in figure 14 yielding the profile depicted in figure 16.

The mean velocity changed as much as 15 percent from frame to frame among the averaged data frames. These changes were not random in location, but a general change in the entire vortex. Not understanding the reason for these variations, the analog video was viewed. The video showed a stable vortex flow field with the expected turbulent variation. That is, until the video was played in slow motion. The vortex was very stable with little turbulence; however, every ten frames an entire vortex would increase velocity indicating a surging flow. The two vortices did not surge together, but oscillated in a phased pattern. Investigating the streamwise standard deviation measurements acquired by the laser velocimeter, shown in figure 17, indicates levels that could be attributable to the flow surges found with the DGV.

Summary

The Doppler global velocimeter has been presented and shown to have the potential to provide global, multicomponent measurements in real time. A prototype DGV has been constructed including custom digital and real time analog signal processing electronics. Laboratory testing of the DGV to measure the velocity field of a rotating wheel and a small subsonic jet flow clearly illustrates its potential. This potential is demonstrated when the DGV was moved to the Basic Aerodynamic Research Tunnel and used to measure the vortical flow field above a 75 degree delta wing. The measurements compare in form with the mean velocity measurements previously acquired by a 5-hole probe and a laser velocimeter. The advantages of the real time capabilities of the DGV were illustrated by its ability to resolve velocity surges in the vortex flow field.

References

Huffaker, R.M.; Fuller, C.E.; and Lawrence, T.R.: *Application of Laser Doppler Velocity Instrumentation to the Measurement of Jet Turbulence*, International Automotive Engineering Congress, Society of Automotive Engineers, Detroit, MI, January 13-17, 1969.

Komine, H.; Brosnan, S.J.; Litton, A.B.; and Stappaerts, E.A.: *Real-Time, Doppler Global Velocimetry*, AIAA 29th Aerospace Sciences Meeting, Reno, NV, paper AIAA-91-0337, January 7-10, 1991.

Meyers, J.F.; and Hepner, T.E.: *Measurement of Leading Edge Vortices from a Delta Wing Using a Three Component Laser Velocimeter*, AIAA 15th Aerodynamic Testing Conference, San Diego, CA, paper AIAA-88-2024, May 18-20, 1988.

Seiler, F.; and Srulijes, J.: *Doppler-Pictures of Velocity Fields, An Application to Fluid Mechanics*, Proceedings of the Third International Symposium on Applications of Laser Anemometry to Fluid Mechanics, Lisbon, Portugal, paper 19.1, July 7-9, 1986.

Self, S.A.: *Laser Doppler Anemometer for Boundary Layer Measurements in High Velocity, High Temperature MHD Channel Flows*, Proceedings of the Second International Workshop on Laser Velocimetry, Purdue University, Vol. II, pp. 44-67, March 27-29, 1974.

Sellers, W.L., III; and Kjelgaard, S.O.: *The Basic Aerodynamics Research Tunnel - A Facility Dedicated to Code Validation*, AIAA 15th Aerodynamic Testing Conference, San Diego, CA, paper AIAA-88-1997, May 18-20, 1988.

Yeh, Y.; and Cummins, H.Z.: *Localized Fluid Flow Measurements with a He-Ne Laser Spectrometer*, *Applied Physics Letters*, Vol. 4, No. 10, pp. 176-78, May 1964.

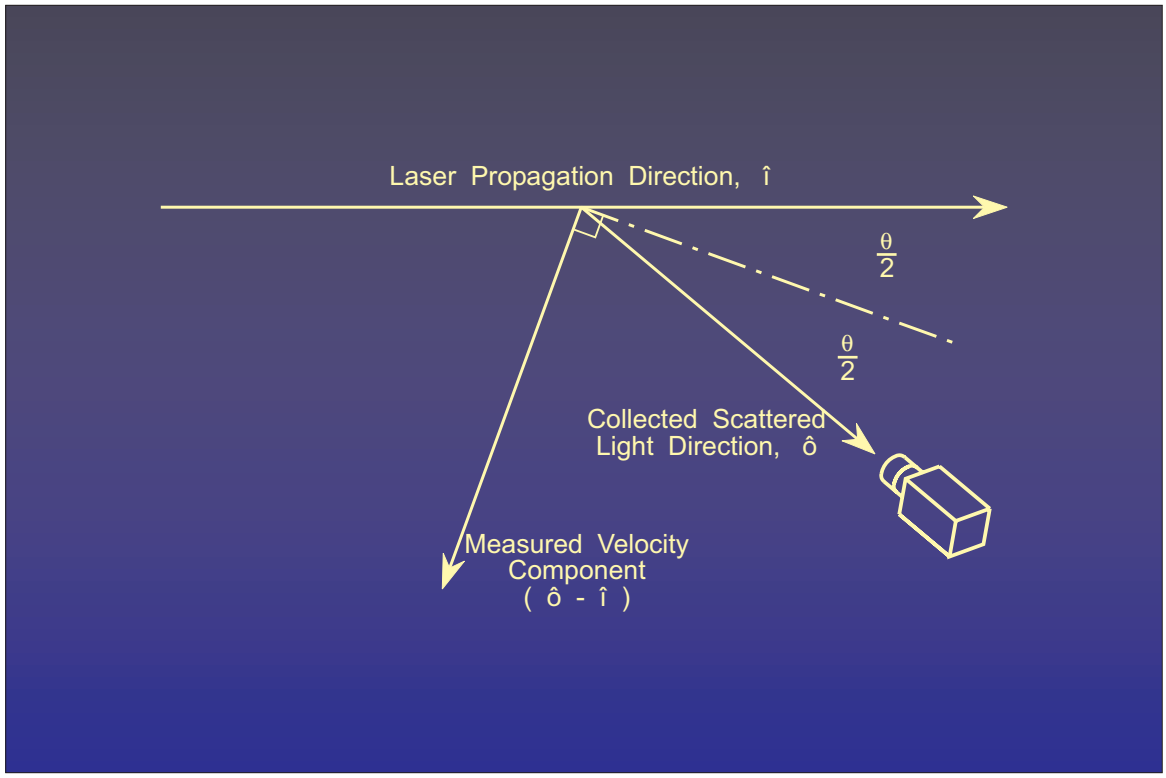

Figure 1.- Determination of measured velocity component direction based on light sheet propagation and receiver location.

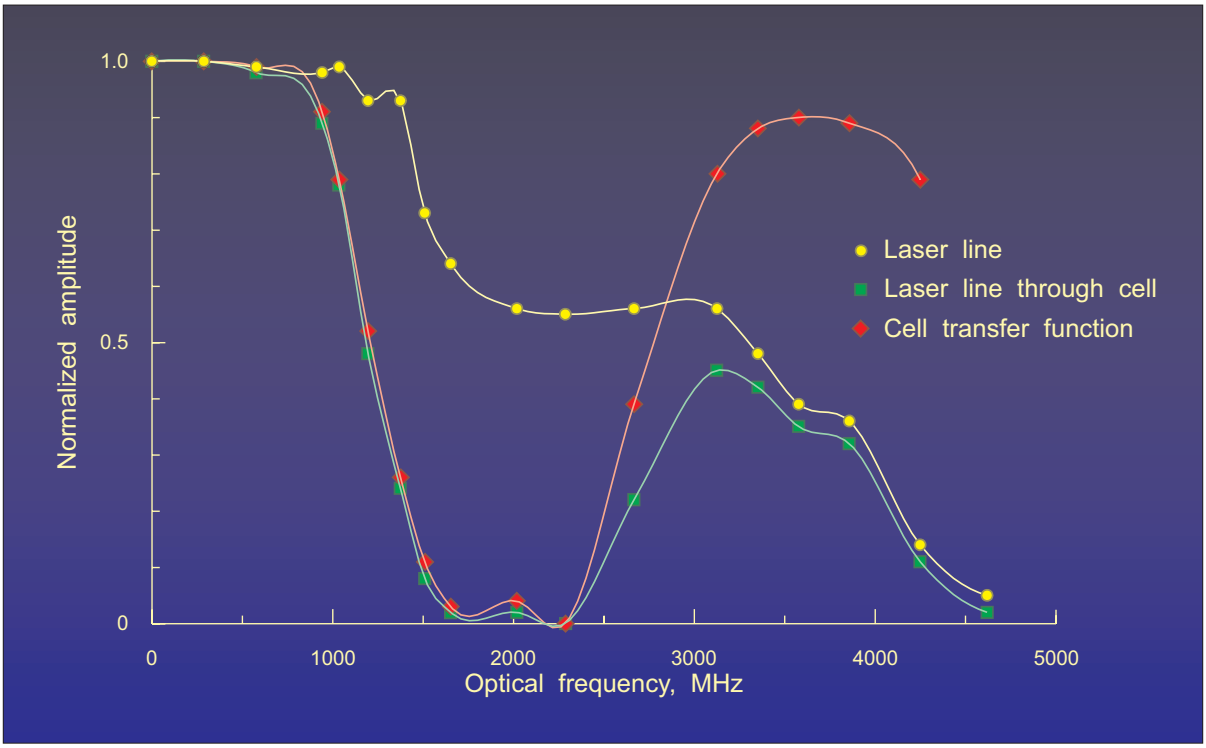

Figure 2.- Transfer function of the Iodine absorption line filter, ALF.

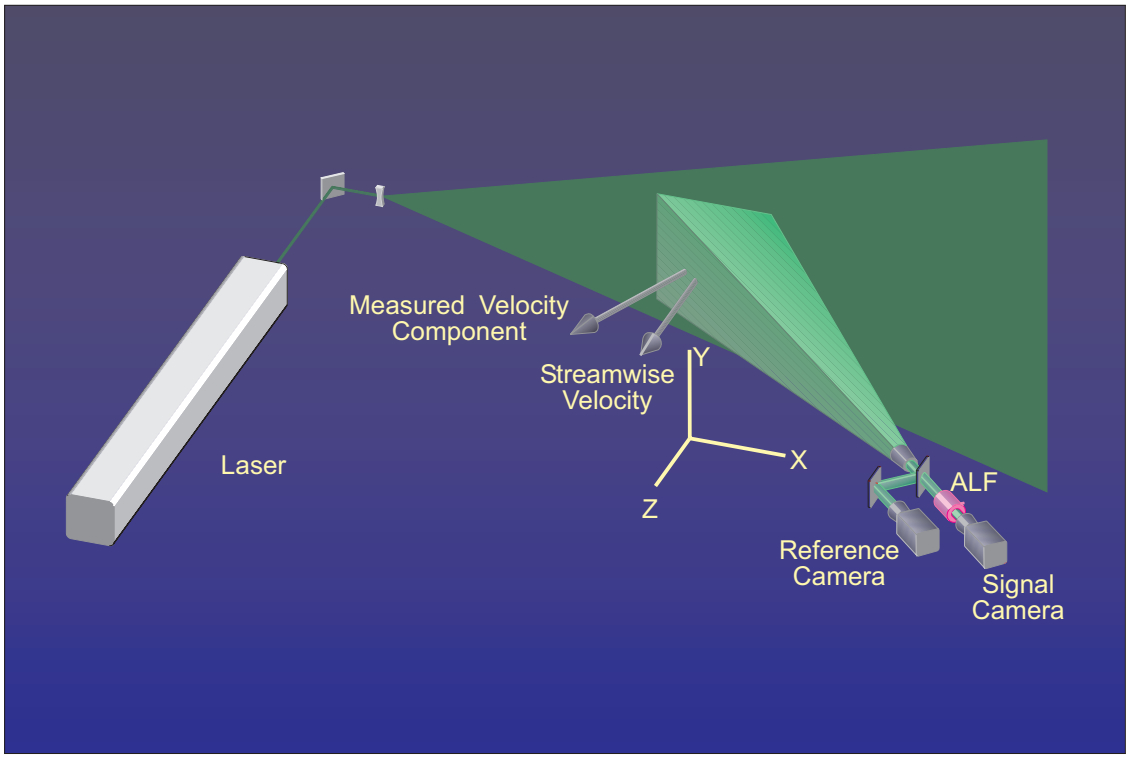

Figure 3.- Graphical representation of the Doppler global velocimeter in the Basic Aerodynamic Research Tunnel, BART.

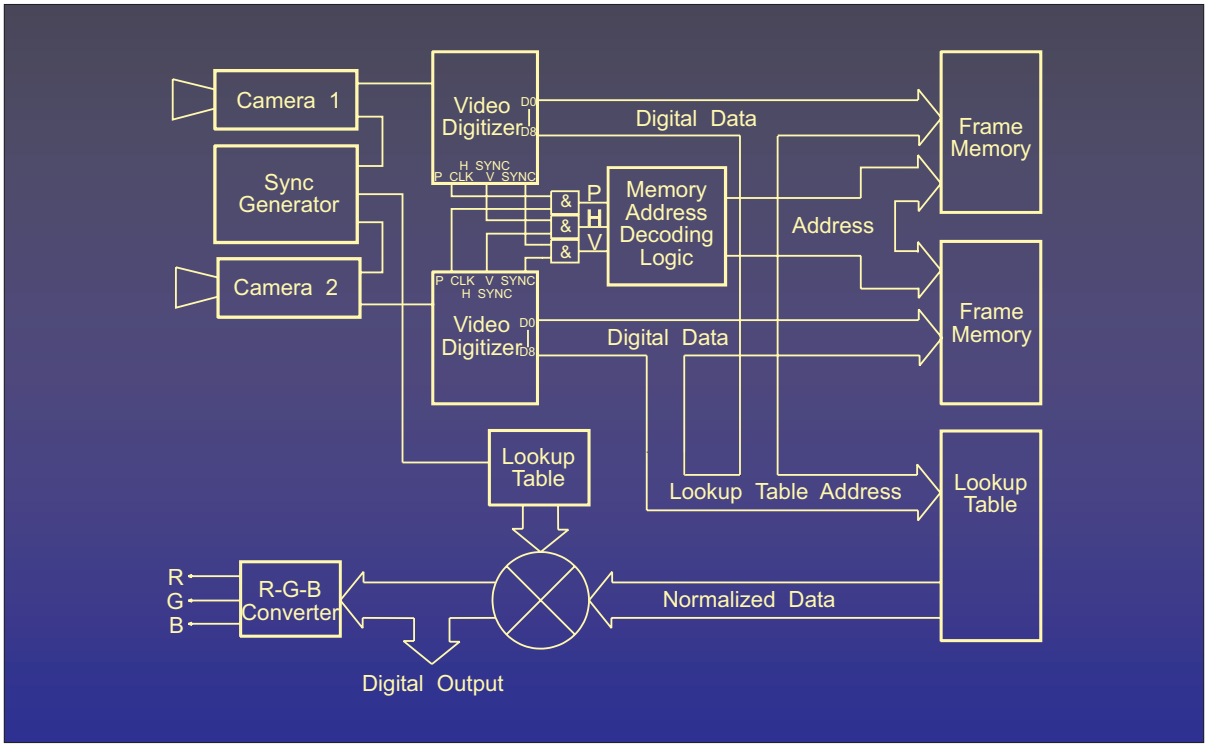

Figure 4.- Block diagram of the digital dual frame grabber for acquiring and processing the images from the reference and signal cameras.

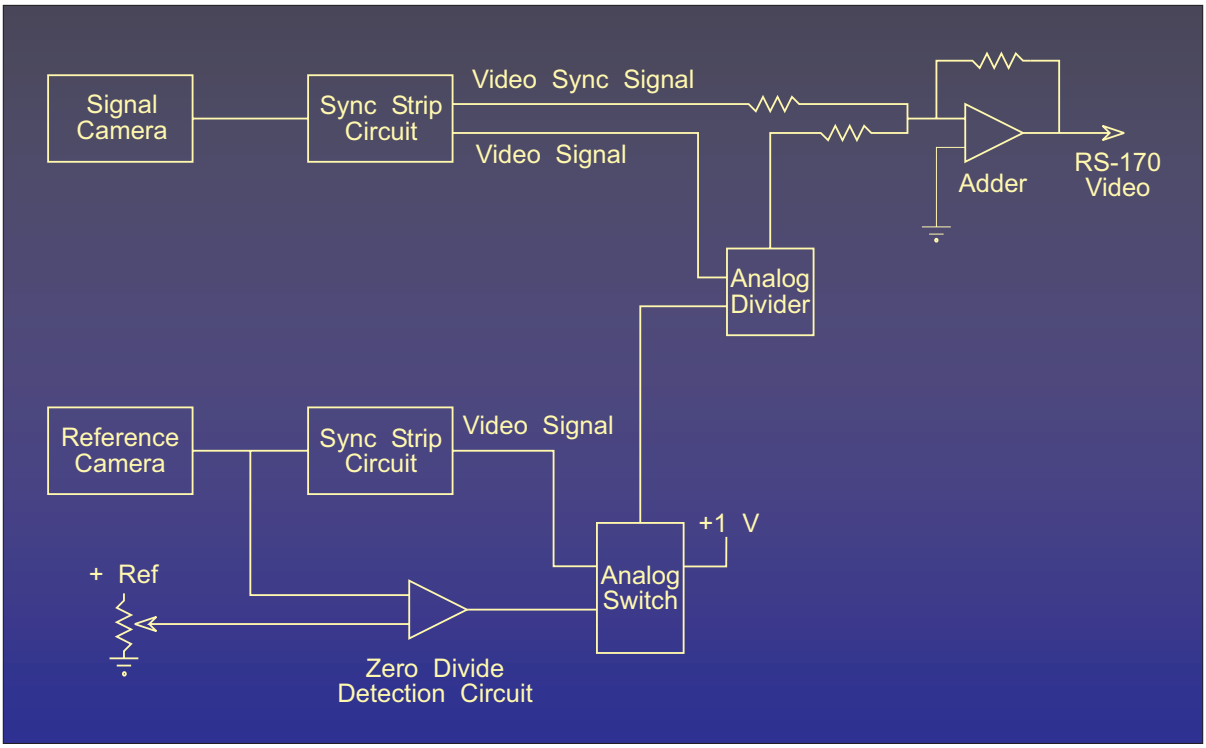

Figure 5.- Block diagram of the analog normalization circuit to normalize the signal image by the reference image in real time.

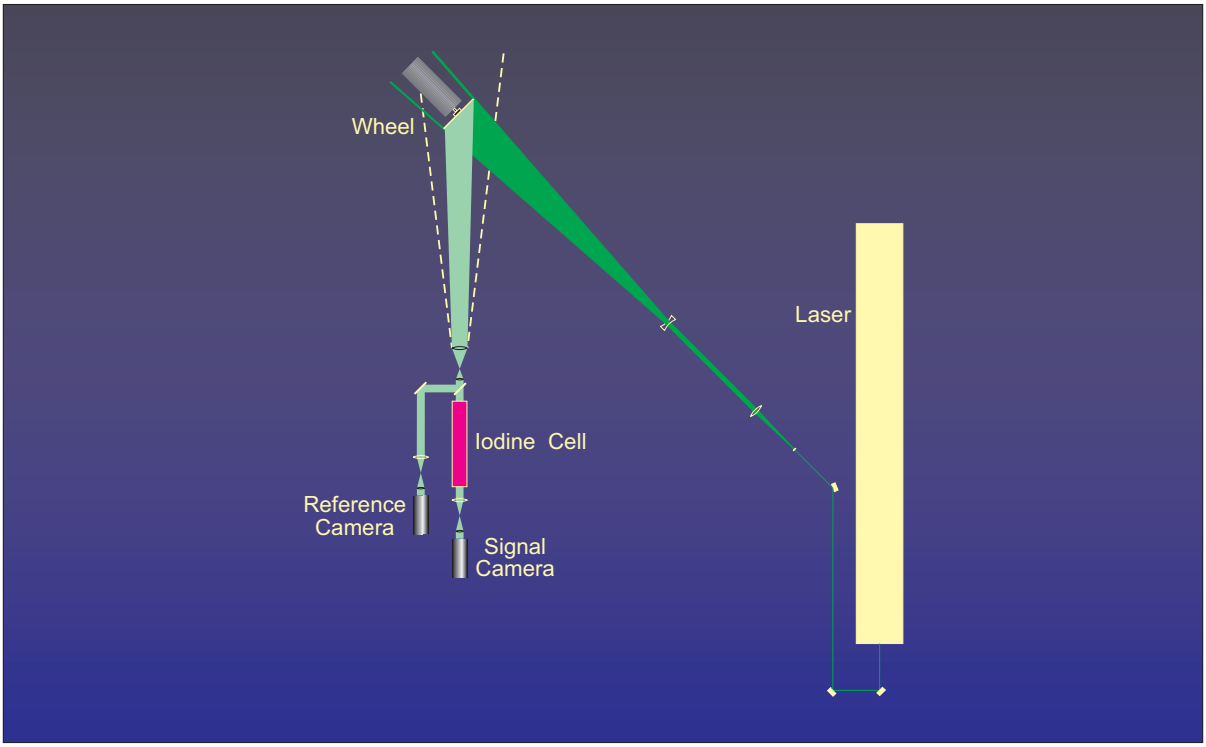

Figure 6.- Graphical representation of the DGV layout for measuring the velocity field from a spinning wheel.

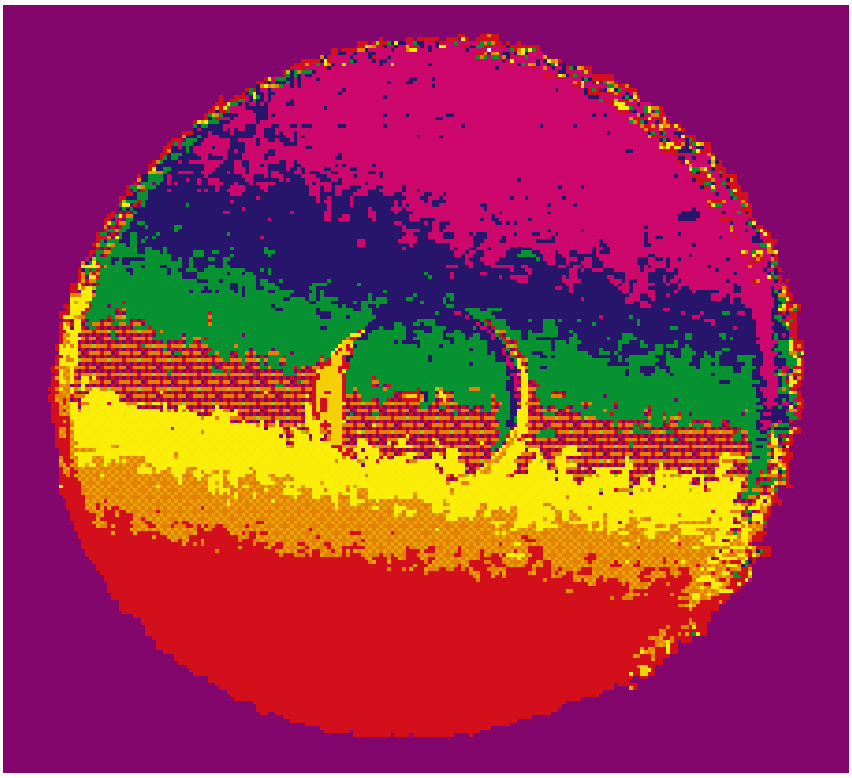

Figure 7.(a)- Gray scale view of the normalized velocity data from the spinning wheel.

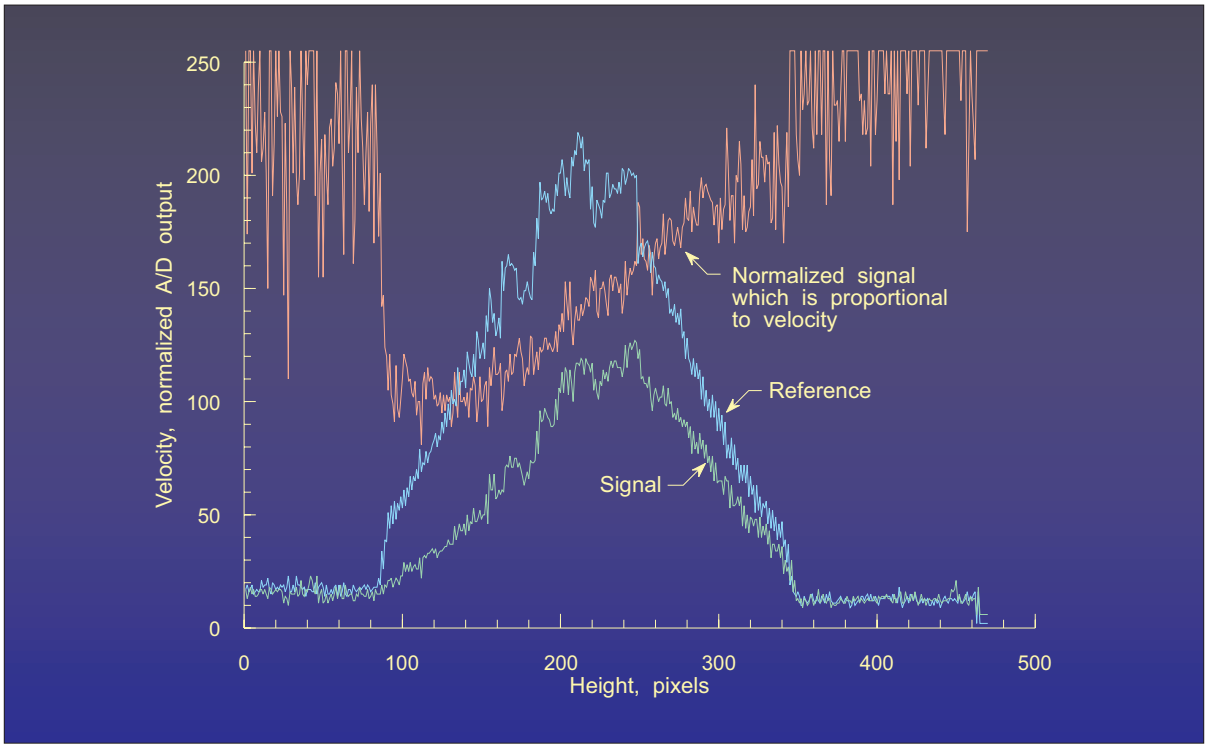

Figure 7.(b)- Velocity profile along the vertical diameter of the wheel.

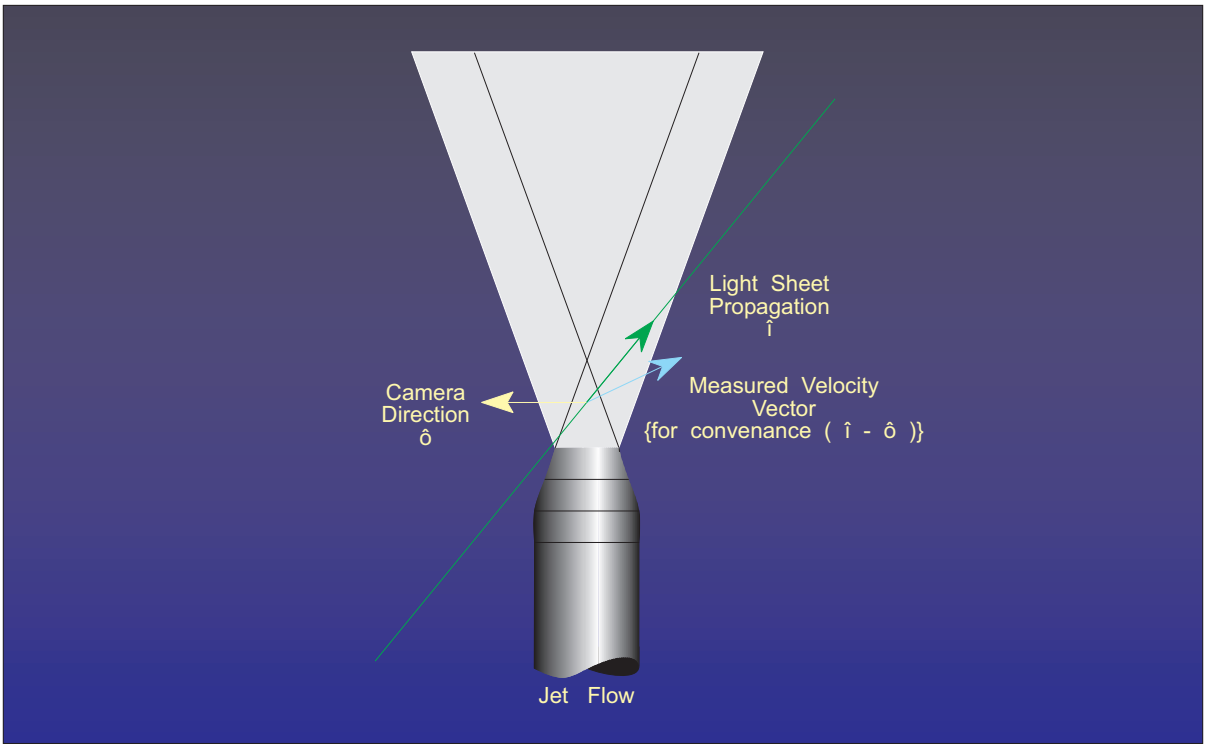

Figure 8.- Graphical representation of the location of the light sheet and receiver for measuring the flow field within a subsonic jet.

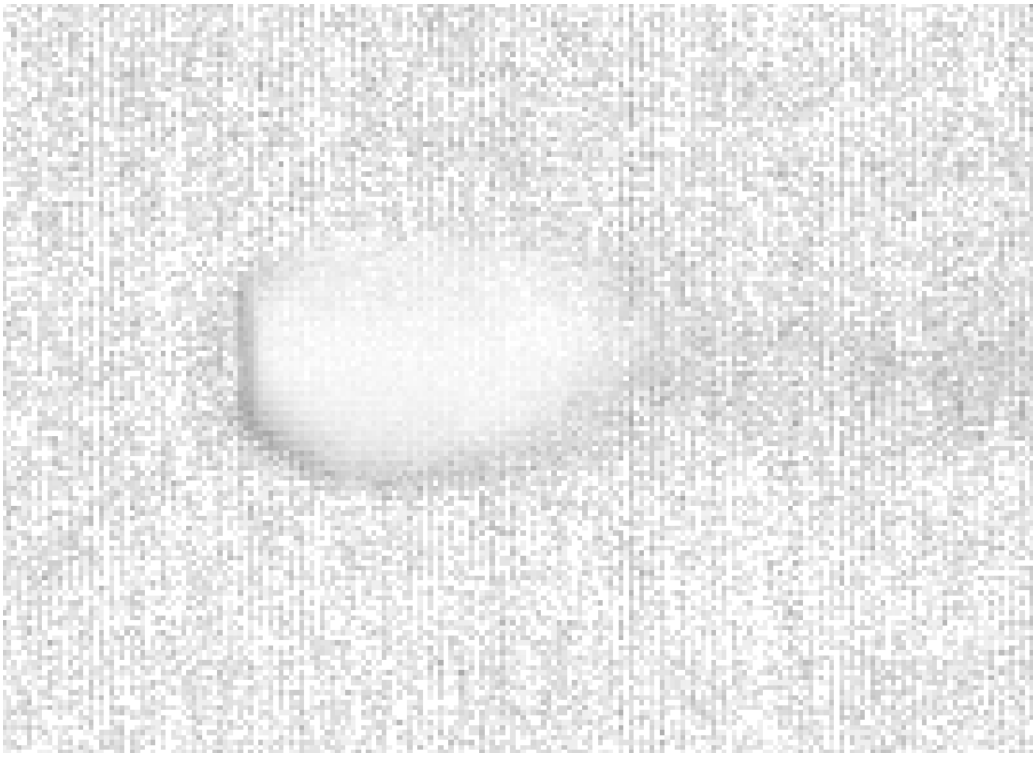

Figure 9.(a)- Gray scale view of the normalized velocity data from the subsonic jet.

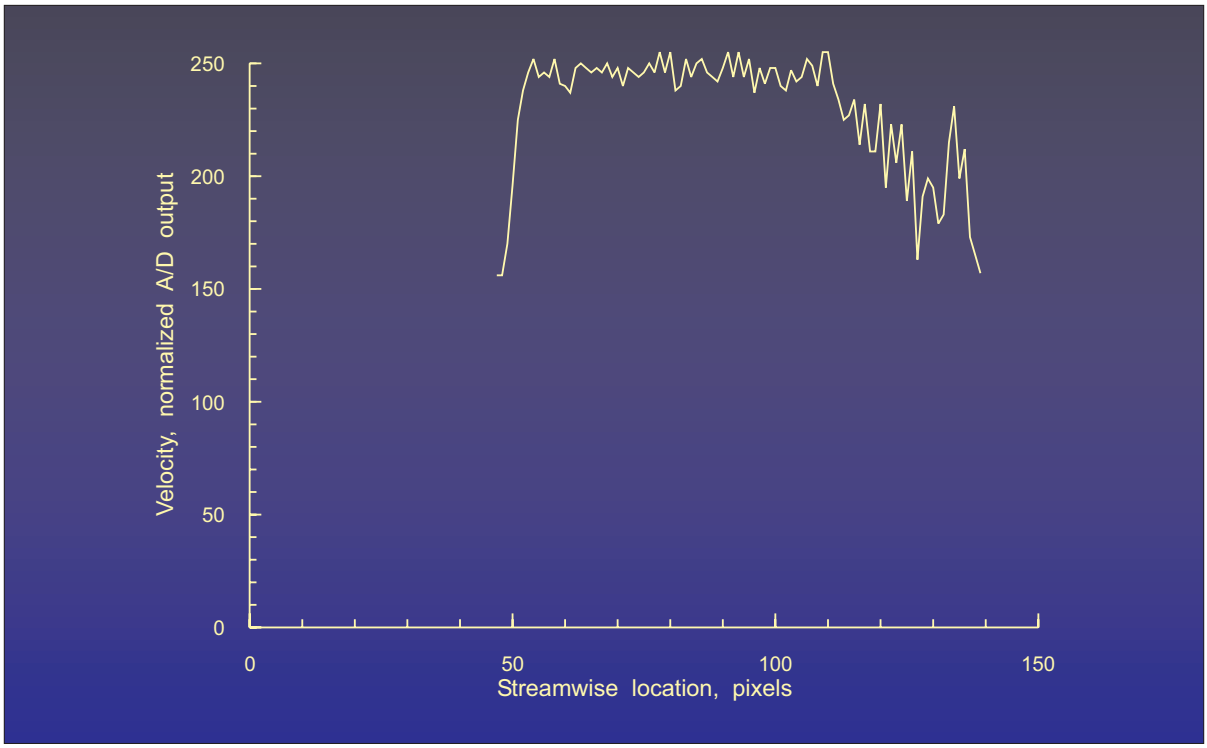

Figure 9.(b)- Velocity profile along the horizontal centerline of the subsonic jet.

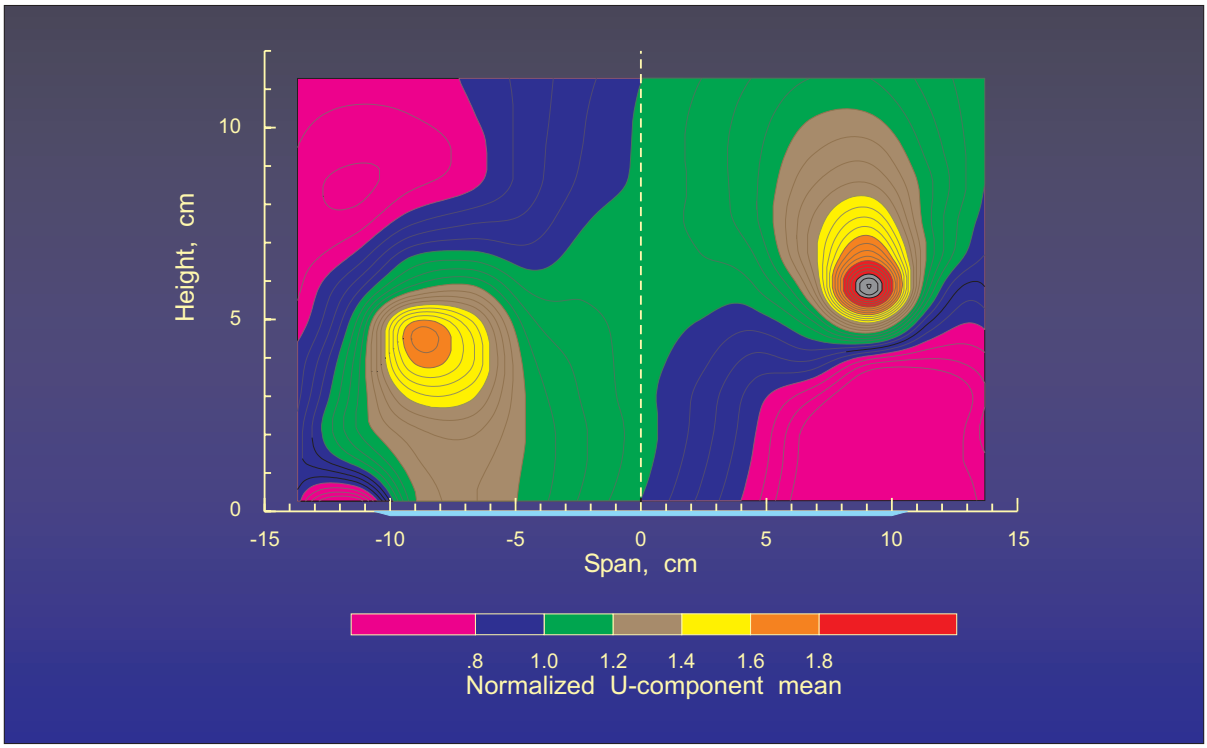

Figure 10.- Velocity contour map of the vortex flow field above a delta wing at 20.5^{o} angle of attack, velocity component is 26.5^{o} from the streamwise direction in the horizontal plane - 5-hole probe measurements.

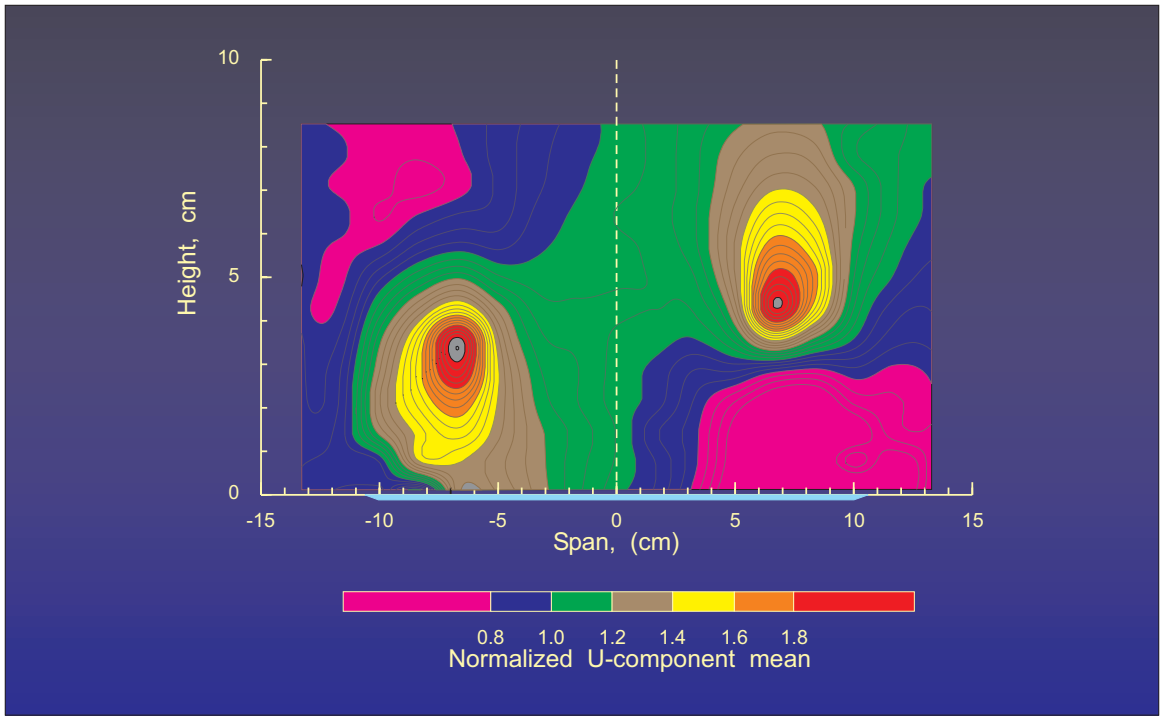

Figure 11.- Velocity contour map of the vortex flow field above a delta wing at 20.5^{o} angle of attack, velocity component is 26.5^{o} from the streamwise direction in the horizontal plane - laser velocimeter measurements.

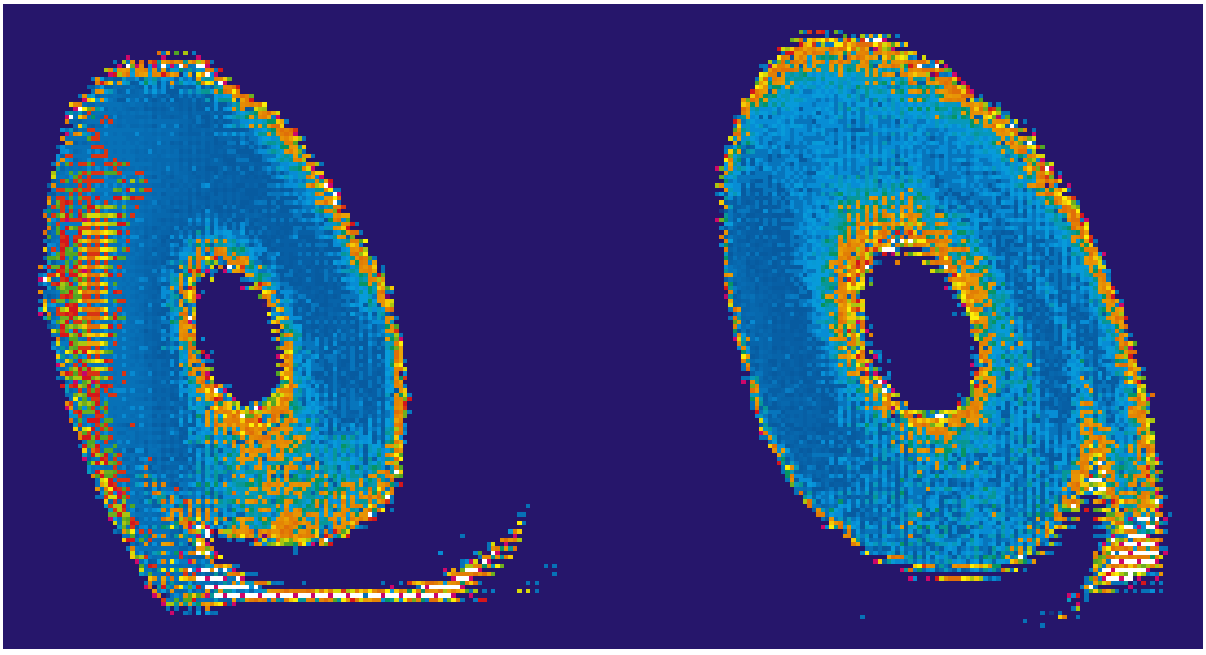

Figure 12.- Single frame velocity contour map of the vortex flow field above a delta wing at 20.5^{o} angle of attack, velocity component is 26.5^{o} from the streamwise direction in the horizontal plane - Doppler global velocimeter measurements.

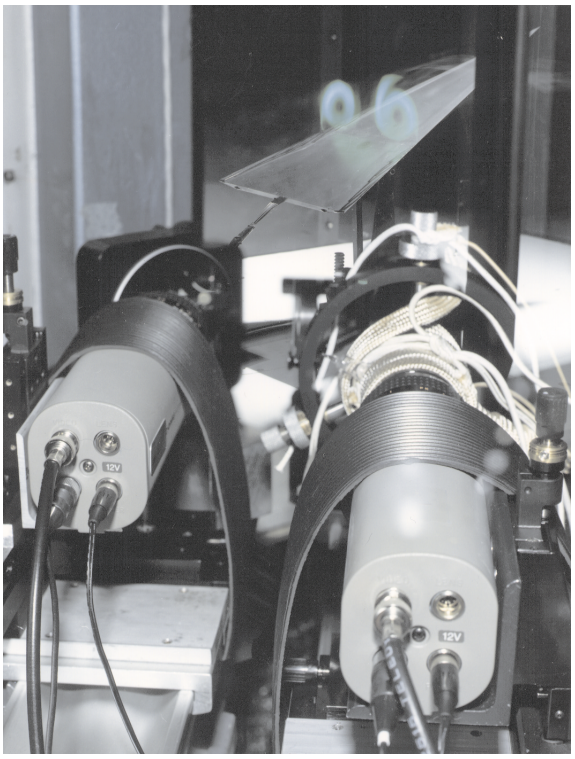

Figure 13.- View of the laser light sheet above the delta wing from the receiver optics location.

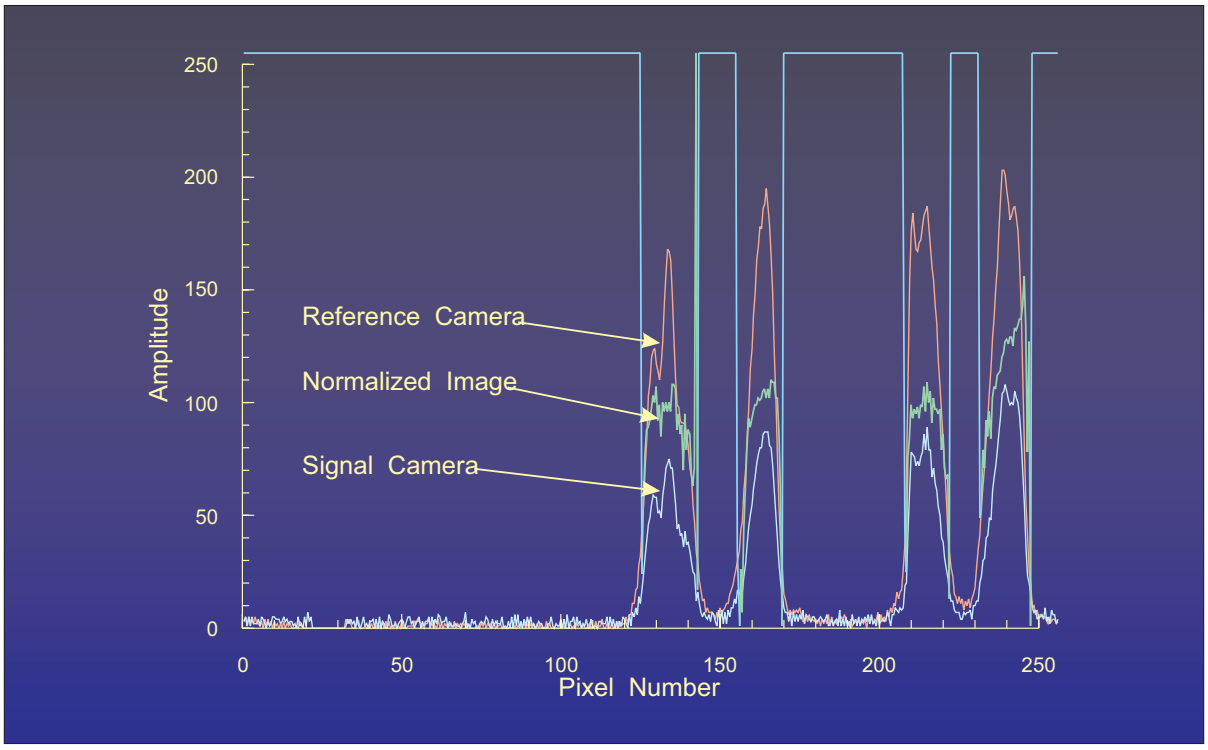

Figure 14.- Signal camera and reference camera signals and their ratio along a horizontal line passing through the center of the vortices, single frame.

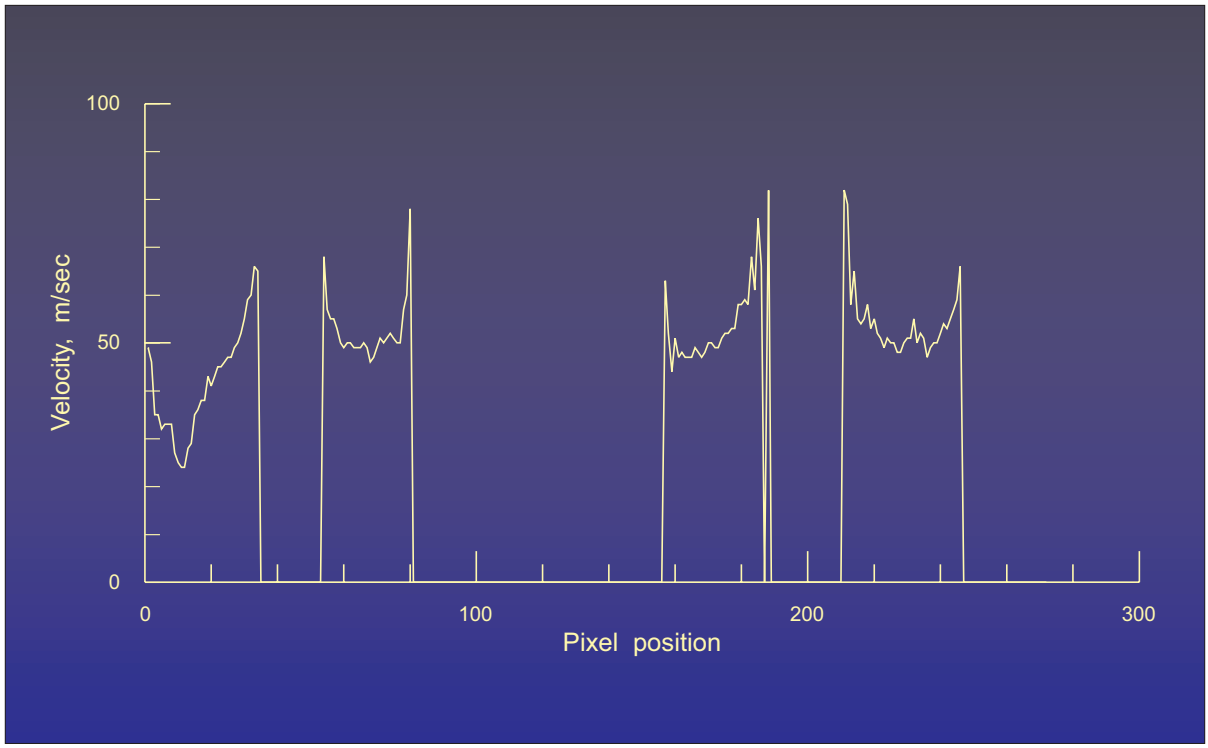

Figure 15.- Normalized signal amplitude along a horizontal line passing through the center of the vortices, average of 10 frames.

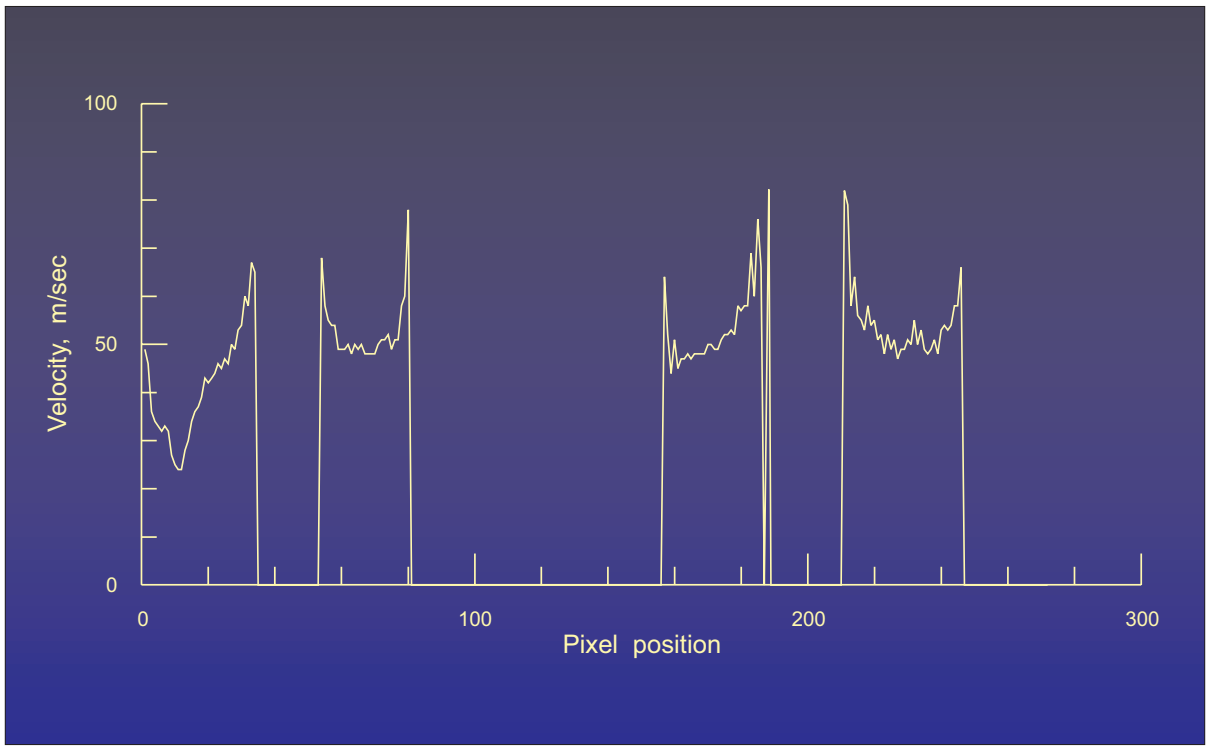

Figure 16.- Normalized signal amplitude with sensitivity variations removed along a horizontal line passing through the center of the vortices, single frame.

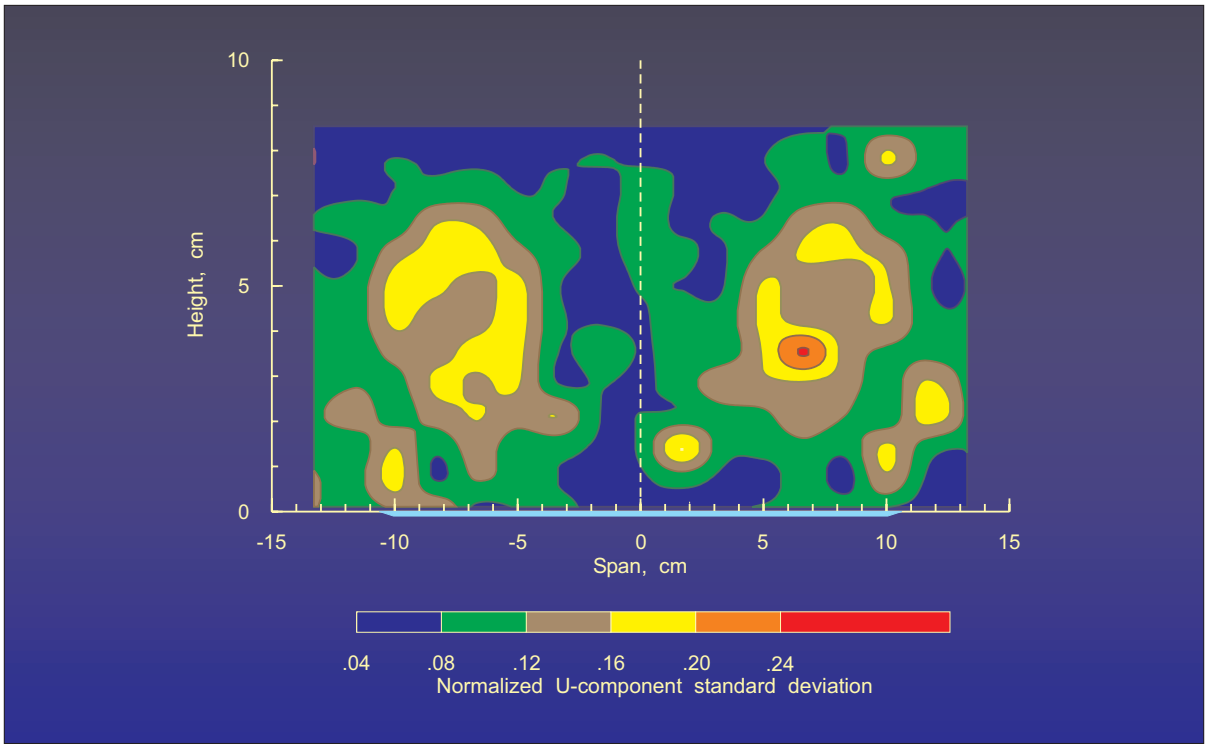

Figure 17.- Normalized streamwise velocity standard deviation contour map of the vortex flow field above a delta wing at 20.5^{o} angle of attack - laser velocimeter measurements.